0026-895X/98/050862-08$3.00/0

MOLECULAR PHARMACOLOGY, **53:**862–869 (1998).

Guanine Nucleotide-Sensitive Inhibition of L-Type Ca^{2+} Current by Lysosphingolipids in RINm5F Insulinoma Cells

HERBERT M. HIMMEL, DAGMAR MEYER ZU HERINGDORF, BERND WINDORFER, CHRIS J. VAN KOPPEN, URSULA RAVENS, and KARL H. JAKOBS

Institut für Pharmakologie, Universitätsklinikum Essen, D-45122 Essen, Germany (H.M.H., D.M. zu H., B.W., C.J. van K., U.R., K.H.J.) and Institut für Pharmakologie und Toxikologie, Technische Universität Dresden, D-01109 Dresden, Germany (H.M.H., U.R.)

Received April 30, 1997; Accepted January 21, 1998

This paper is available online at http://www.molpharm.org

ABSTRACT

The lysosphingolipids sphingosine-1-phosphate (SPP) and sphingosylphosphorylcholine (SPPC) reportedly increase free cytosolic Ca^{2+} concentration ($[Ca^{2+}]_i$) in a variety of cell types, apparently by activating G protein-coupled plasma membrane receptors. We investigated whether and how sphingolipids modulate Ca^{2+} homeostasis in the insulinoma cell line RINm5F. The addition of SPPC and glucopsychosine (GPS) did not affect basal $[Ca^{2+}]_i$ but inhibited the KCl (30 mM)-induced increase in $[Ca^{2+}]_i$ in a pertussis toxin-insensitive and concentration-dependent manner ($EC_{50} \sim 5$ μM). Similar inhibitory effects were observed with dihydro-SPPC and psychosine, whereas SPP and various *N*-acylated sphingolipids (at 10 μM each) had little or no effect on the KCl-induced $[Ca^{2+}]_i$ increase. Because in RINm5F cells the primary pathway for depolarization-induced $[Ca^{2+}]_i$ increase are L-type Ca^{2+} channels, we studied whether sphingolipids reduce L-type Ca^{2+} current ($I_{Ca.L}$). When added to the bath, GPS and SPPC, but not SPP (10 μM each), rapidly reduced maximal $I_{Ca.L}$ by ~35%, similar to the α_2-adrenoceptor agonist clonidine (30 μM). However, when applied internally, GPS had no effect on $I_{Ca.L}$. When the electrode solution contained the stable GDP analog guanosine-5′-*O*-(2-thio)diphosphate (1 and 10 mM), the inhibitory effect of GPS was abolished. In conclusion, a novel cellular action of lysosphingolipids is observed in RINm5F cells (i.e., a guanine nucleotide-sensitive inhibition of L-type Ca^{2+} currents). The pharmacological profile of this inhibition is unique and unlike any known lysosphingolipid receptor-mediated action.

Products of sphingolipid metabolism can modulate various cellular functions, such as cell growth and DNA synthesis, as well as programmed cell death (for review see Spiegel *et al.*, 1996). An intracellular second messenger role of sphingolipids, particularly of SPP, for cellular Ca^{2+} homeostasis is supported by the demonstration that SPP can mobilize Ca^{2+} from intracellular stores (Ghosh *et al.*, 1994; Mattie *et al.*, 1996) and by the finding that cellular SPP levels increase on activation of platelet-derived growth factor and FcεRI antigen receptors (Olivera and Spiegel, 1993; Choi *et al.*, 1996).

In addition to their role as intracellular messengers, sphingolipid compounds apparently bind to and activate PTX-sensitive G protein-coupled plasma membrane receptors in a variety of cell types. The strongest evidence for the existence of a specific sphingolipid receptor emerged from studies on muscarinic K^+ currents in guinea pig atrial myocytes. Both SPP and SPPC, at similar nanomolar concentrations, activated K^+ currents in a strictly GTP- and PTX-sensitive manner, but only when applied to the extracellular face (Bünemann *et al.*, 1996; van Koppen *et al.*, 1996a). Furthermore, exogenously added SPP and SPPC have been reported to cause a rapid PTX-sensitive increase in $[Ca^{2+}]_i$ in various cell types (Okajima and Kondo, 1995; Meyer zu Heringdorf *et al.*, 1996, 1997; Spiegel *et al.*, 1996; van Koppen *et al.*, 1996a, 1996b). In contrast to the activation of cardiac K^+ currents by SPP and SPPC, SPP was generally more potent than SPPC to increase $[Ca^{2+}]_i$ in intact cells. For example, in HEK 293 and bovine aortic endothelial cells, nanomolar concentrations of SPP led to a rapid increase in $[Ca^{2+}]_i$, whereas micromolar concentrations of SPPC were required to elicit a similar response (Meyer zu Heringdorf *et al.*, 1996; van Koppen *et al.*, 1996a). Finally, in human leukemia HL-60 cells, only SPPC,

This work was supported by Grant 0310493A from Bayer AG and the Bundesministerium für Bildung and Wissenschaft, Forschung und Technologie and the Juterne Forschungsförderung Essen program of the Universitätsklinikum Essen.

Preliminary results have been published in abstract form: Himmel HM, Meyer zu Heringdorf D, Windorfer B, van Koppen CJ, Ravens U, and Jakobs KH (1997) Sphingolipid receptor-mediated inhibition of L-type Ca^{2+} current in the insulinoma cell line RINm5F. *Naunyn-Schmiedebergs Arch Pharmacol* **355:**R52.

H.M.H. and D.M.z.H. contributed equally to this work.

ABBREVIATIONS: SPP, sphingosine-1-phosphate; $[Ca^{2+}]_i$, cytosolic free Ca^{2+} concentration; GDPβS, guanosine-5′-*O*-(2-thio)diphosphate; GPS, glucopsychosine; GTPγS, guanosine-5′-*O*-(3-thio)triphosphate; HEK, human embryonic kidney; HEPES, 4-(2-hydroxyethyl)-1-piperazineethanesulfonic acid; $I_{Ca.L}$, L-type Ca^{2+} current; PKC, protein kinase C; PS, psychosine; PTX, pertussis toxin; SPPC, sphingosylphosphorylcholine; EGTA, ethylene glycol bis(β-aminoethyl ether)-*N*,*N*,*N*′,*N*′-tetraacetic acid.

at micromolar concentrations, elevated $[Ca^{2+}]_i$, whereas SPP was ineffective (van Koppen *et al.*, 1996b). Based on these observations, the existence of distinct sphingolipid receptor subtypes with different ligand profiles has been suggested (Bünemann *et al.*, 1996; Meyer zu Heringdorf *et al.*, 1997).

Because an increase in $[Ca^{2+}]_i$ is an important prerequisite for exocytosis and insulin secretion in pancreatic β cells (Sharp, 1997), we investigated whether sphingolipids modulate Ca^{2+} homeostasis in the rat insulinoma cell line RINm5F. For this, various sphingolipids were studied on basal and depolarization-induced $[Ca^{2+}]_i$ increase in intact cells and on membrane Ca^{2+} currents. We report that certain sphingolipids markedly inhibit depolarization-induced $[Ca^{2+}]_i$ increase in RINm5F cells, without affecting basal $[Ca^{2+}]_i$, and inhibit L-type Ca^{2+} currents in a guanine nucleotide-sensitive manner.

Experimental Procedures

Materials. SPP was purchased from BIOMOL (Hamburg, Germany). All other sphingolipids were obtained from Matreya (Bad Homburg, Germany). The sphingolipids were dissolved in methanol and stored at −20°. Aliquots were dried in a SpeedVac concentrator before use and redissolved in 1 mg/ml bovine serum albumin. Clonidine, nifedipine, verapamil, GTP, GTPγS, and GDPβS (trilithium salt) were from Sigma (Deisenhofen, Germany). None of the solvents used for the various compounds influenced measurements of $[Ca^{2+}]_i$ or membrane currents. All other materials were from previously described sources (Meyer zu Heringdorf *et al.*, 1996; van Koppen *et al.*, 1996a).

Cell culture. RINm5F insulinoma cells were cultured in RPMI-1640 medium containing 10% fetal calf serum, 100 units/ml penicillin G, and 0.1 mg/ml streptomycin. HEK 293 cells stably expressing the human cardiac L-type Ca^{2+} channel α_{1C} subunit together with a β_3 subunit (Klöckner *et al.*, 1997) were cultured in Dulbecco's modified Eagle's medium supplemented with 10% fetal calf serum, 100 units/ml penicillin G, 0.1 mg/ml streptomycin, and 0.6 mg/ml G418. For current measurements, cells were plated at low density onto thin glass coverslips and used on the following day. Pretreatment with PTX was performed for 16–20 hr with 100 ng/ml of the toxin.

$[Ca^{2+}]_i$ measurements. $[Ca^{2+}]_i$ was quantified spectrofluorimetrically (LS 5 B; Perkin-Elmer Cetus, Norwalk, CT, or F2000; Hitachi, Yokohama, Japan) with the fluorescent dye Fura-2 as described previously (Meyer zu Heringdorf *et al.*, 1996; van Koppen *et al.*, 1996a). RINm5F cells were harvested after mild trypsin treatment, resuspended in culture medium, and incubated with 1 μM Fura-2/AM for 60 min at room temperature. To remove excess Fura-2/AM, cells were washed twice and resuspended at a density of 10^6 cells/ml. $[Ca^{2+}]_i$ was measured at room temperature in a continuously stirred cell suspension, with alternating excitation wavelengths between 340 nm and 380 nm while fluorescence emission was read at 495 nm. For measurements in the absence of extracellular Ca^{2+}, cells were resuspended in Ca^{2+}-free buffer immediately before start of the experiment, and EGTA (50 μM) was added 30 sec before KCl.

Electrophysiology. Cells were grown on glass coverslips that were mounted in a custom-made chamber placed on the stage of an inverted microscope (Axiovert 10; Carl Zeiss, Oberkochen, Germany). The chamber was continuously perfused at a constant rate (1.2 ml/min). The single-electrode voltage-clamp technique was applied to measure membrane potential and membrane current. Fire-polished pipettes from borosilicate filament glass (Hilgenberg, Malsfeld, Germany; o.d., 1.5 mm) were used to form GΩ seals with gentle suction. The patched membrane then was disrupted by a pulse of suction to establish continuity of the interior of the electrode with the cytosol. Voltage-clamp or current-clamp was achieved using an Axon 200 amplifier. For stimulus protocol design and data acquisition, the Axolab TL-125 interface and pClamp 5.5 software (Axon Instruments, Foster City, CA) were used.

$I_{Ca.L}$ was measured with Ba^{2+} as charge carrier at room temperature (22–25°). The bath was perfused with a solution composed of 137 mM NaCl, 5.4 mM CsCl, 10 mM $BaCl_2$, 1.25 mM $MgCl_2$, 10.0 mM HEPES, and 10.0 mM glucose (pH 7.4 adjusted with NaOH). The tip resistances of the pipettes were 3–4 MΩ when filled with a solution composed of 140 mM CsCl, 4.0 mM $MgCl_2$, 10.0 mM EGTA, 10.0 mM HEPES, and 4.0 mM Na_2-ATP (pH 7.3 adjusted with CsOH). Assuming a total $[Ca^{2+}]$ of 10 μM, the free $[Ca^{2+}]$ and free $[Mg^{2+}]$ were 5 nM and 240 μM, respectively (EQCAL; Biosoft, Cambridge, UK).

Characterization of the Ba^{2+} current. Because several types of voltage-activated Ca^{2+} channels may coexist in insulin-secreting cells (for review, see Ashcroft and Rorsman, 1989), conditions were chosen such as to maximize currents through L-type Ca^{2+} channels using Ba^{2+} as charge carrier (de Waard *et al.*, 1996). Under these conditions, sizeable Ba^{2+} currents could be measured in 86% of the 250 patched cells. Starting from the holding potential of −80 mV throughout all experiments, voltage ramps in the range of −100 to +80 mV (duration, 400 msec) activated membrane currents with current-voltage relations typical for $I_{Ca.L}$. No voltage-activated currents were observed negative to −40 mV. In 17% of the cells, voltage ramp-derived current-voltage relations displayed a "hump" in the negative slope region around −20 mV, suggesting the presence of T-type Ca^{2+} channels. The properties of voltage ramp-derived current-voltage relations were identical to those obtained by voltage steps (range, −60 to +60 mV; increments, 10 mV; duration, 300 msec). Currents activated positive to −40 mV, peaked at +3 ± 1 mV, and reversed at +49 ± 1 mV; conductance was half-maximal at −10 ± 1 mV with a respective slope factor of +6 ± 3 mV (mean ± standard error, 18 experiments). A standard double-pulse protocol was applied to test Ca^{2+} channel availability, which was half-maximal at −17 ± 2 mV (slope factor, −11 ± 1 mV, mean ± standard error; 26 experiments; data not shown).

Measurements of time-dependent changes of $I_{Ca.L}$ indicated that after disruption of the membrane, dialysis of the cell interior was completed within 3 min, and thereafter, current amplitudes remained stable for ~10 min. Thus, "run-down" of I_{Ca} was considered negligible within this period of time.

Specific blockers of L-type Ca^{2+} channels [i.e., the dihydropyridine nifedipine (5 μM) and the phenylalkylamine verapamil (50 μM), as well as Cd^{2+} (200 μM)] greatly reduced or even abolished Ba^{2+} currents. Compared with cardiac or smooth muscle cells, high concentrations of organic Ca^{2+} channel blockers are usually required in pancreatic β cells, particularly when stimulated at the low rate of 0.1 Hz (Findlay and Dunne, 1985; Ashcroft and Rorsman, 1989), which may be due to the nonidentical channel-forming α_1 subunits of cardiac/smooth muscle type (α_{1C}) and neuroendocrine-type (α_{1D}) L-type Ca^{2+} channels (Birnbaumer *et al.*, 1994).

Membrane potential measurements. Membrane potential measurements in current-clamp mode were performed with a bath solution composed of 150 mM NaCl, 5.4 mM KCl, 1.8 mM $CaCl_2$, 2.0 mM $MgCl_2$, 10.0 mM HEPES, and 10.0 mM glucose (pH 7.4 adjusted with NaOH). Electrodes were filled with a solution consisting of 140 mM KCl, 4.0 mM $MgCl_2$, 5.0 mM $CaCl_2$, 10.0 mM EGTA, 10.0 mM HEPES, and 4.0 mM Na_2-ATP (pH 7.3 adjusted with KOH). Assuming a total $[Ca^{2+}]$ of 10 μM, free $[Ca^{2+}]$ and free $[Mg^{2+}]$ were 50 nM and 300 μM, respectively (EQCAL; Biosoft).

Data analysis and statistics. Conductance curves for I_{Ca} were estimated by dividing current amplitude at different potentials (V_m) by the corresponding driving force $V_m - V_{rev}$, where V_{rev} is the reversal potential determined by linear regression from the positive slope region of individual current-voltage curves. A Boltzmann function of the form

$$g/g_{max} = 1/[1 + \exp((V_m - V_{0.5})/k)]$$

was fitted to the data points for calculation of potentials of half-maximum activation $V_{0.5}$ and slope factors k. Steady state inactiva-

tion curves for I_{Ca} were fitted in a similar manner using normalized current data. Curve fitting was performed with pClamp software (Clampfit) or Prism (GraphPAD Software, San Diego, CA).

The results were expressed as mean ± standard error. Differences between two sets of data were analyzed by means of Student's *t* test for paired or grouped data and considered significant at $p < 0.05$. Three and more sets of data were analyzed with analysis of variance followed by Tukey-Kramer multiple comparisons test. Whenever parametric tests were inappropriate, nonparametric tests according to Mann-Wilcoxon-Whitney or Kruskal-Wallis were applied.

Results

Inhibition of KCl-induced $[Ca^{2+}]_i$ increase in RINm5F cells by lysosphingolipids. Depolarization of suspended RINm5F cells by the addition of 30 mM KCl rapidly increased $[Ca^{2+}]_i$ by several hundred nanomolar before reaching a new elevated plateau level (Fig. 1A). The addition of SPPC (10 μM) had no effect on basal $[Ca^{2+}]_i$. However, SPPC largely attenuated the increase in $[Ca^{2+}]_i$ elicited by KCl depolarization (Fig. 1B). This inhibitory effect on the KCl-induced increase in $[Ca^{2+}]_i$ was not confined to SPPC but also was observed with dihydro-SPPC, GPS, and PS (Fig. 2A). On the other hand, *N*-acylated sphingolipids (i.e., *N*-acetyl-SPPC, *N*-acetyl-PS, C2-ceramide, and ceramide-1-phosphate), as well as SPP, had little or no effect on the KCl-induced $[Ca^{2+}]_i$ increase. The inhibitory effect of SPPC and GPS was half-maximal at 4.9 ± 1.0 μM (five experiments) and 5.6 ± 0.6 μM (five experiments), respectively (Fig. 2B). Because in other cellular systems, sphingolipid-induced signaling is mediated by G proteins of the G_i family (Okajima and Kondo, 1995; Bünemann *et al.*, 1996; Meyer zu Heringdorf *et al.*, 1996; van Koppen *et al.*, 1996a; 1996b), RINm5F cells were pretreated with PTX (100 ng/ml, 16–20 hr). However, PTX pretreatment affected neither the KCl-induced increase in $[Ca^{2+}]_i$ (Fig. 1C) nor its attenuation by SPPC (Fig. 1D). Similar results were obtained with other lysosphingolipids (data not shown). Thus, the sphingolipids tested did not require G_i-type G proteins for inhibition of KCl-induced $[Ca^{2+}]_i$ transients. Because lysosphingolipids such as PS can inhibit PKC (Hannun and Bell, 1987), the influence of PKC inhibition on $[Ca^{2+}]_i$ transients was tested. Pretreatment of RINm5F cells with the PKC inhibitor staurosporine (100 nM, 30 min) affected neither the KCl-induced $[Ca^{2+}]_i$ increase nor its inhibition by the lysosphingolipid GPS. On the other hand, activation of PKC by phorbol 12-myristate 13-acetate (1 μM, 10 min) reduced the KCl-induced $[Ca^{2+}]_i$ increase and enhanced the inhibitory effect of GPS (data not shown). Thus, inhibition of PKC apparently was not involved in inhibition of $[Ca^{2+}]_i$ transients by lysosphingolipids.

The KCl-induced increase in $[Ca^{2+}]_i$ was caused by influx of Ca^{2+} from the extracellular space because it was prevented by removal of extracellular Ca^{2+} and it was blocked by the L-type Ca^{2+} channel blocker verapamil (IC_{50} = 14 μM, data not shown). Because RINm5F cells express ryanodine receptors (Bennett *et al.*, 1996), we studied whether lysosphingolipids may affect this Ca^{2+} signaling pathway as well. The application of caffeine (40 mM) to control cells and cells pretreated with GPS (10 μM) increased $[Ca^{2+}]_i$ by 40 ± 3 nM (nine experiments) and 39 ± 3 nM (seven experiments), respectively (data not shown). Thus, GPS-induced inhibition of $[Ca^{2+}]_i$ transients in RINm5F cells seems to be restricted to the influx component, leaving ryanodine receptor-mediated Ca^{2+} release apparently unaltered. Inhibition of depolarization-induced Ca^{2+} influx also could be due to hyperpolarizing currents activated by the sphingolipids, with the obvious candidates being the ATP-dependent K^+ current, $I_{K.ATP}$, and the voltage-dependent delayed rectifier current, $I_{K.DR}$ (Ashcroft and Rorsman, 1989; Sharp, 1997). However, in current-clamp experiments, GPS (20 μM) was found to slightly depolarize RINm5F cells, from −58.9 ± 3.1 to −53.7 ± 3.1 mV (four experiments; Fig. 3), whereas the $I_{K.ATP}$ activator diazoxide (100 μM) hyperpolarized the membrane as expected (from −45.6 ± 5.7 to −56.6 ± 4.7 mV; five experiments; data not shown). This finding indicated that hyperpolarization due to activation of $I_{K.ATP}$ did not participate in the inhibitory action of GPS. Furthermore, GPS did

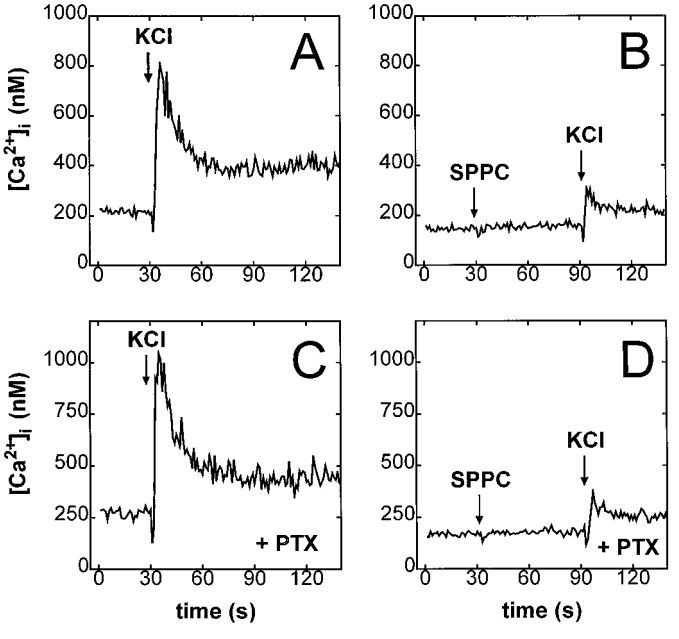

Fig. 1. Influence of SPPC on basal and KCl-induced $[Ca^{2+}]_i$ increase in RINm5F cells. *Tracings* of representative $[Ca^{2+}]_i$ measurements in control (A and B) and PTX-treated (100 ng/ml, 16–20 hr) cells (C and D). A and C, Addition of 30 mM KCl only. B and D, Addition of 10 μM SPPC followed 60 sec later by addition of KCl.

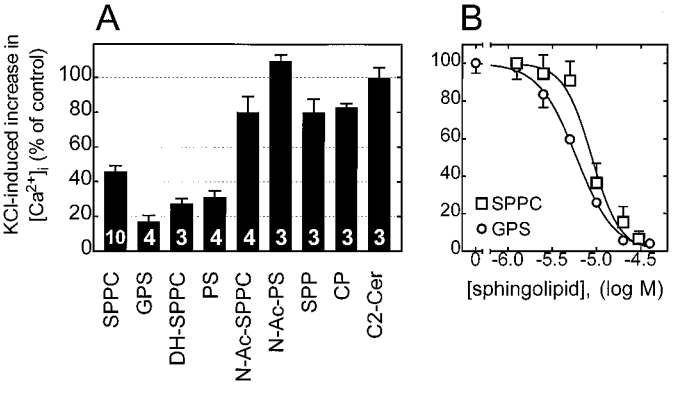

Fig. 2. Influence of various sphingolipids on the KCl-induced $[Ca^{2+}]_i$ increase in RINm5F cells. A, Effects of various sphingolipids (10 μM each) on the KCl (30 mM)-induced $[Ca^{2+}]_i$ increase. Values are mean ± standard error relative to controls, in which KCl-induced $[Ca^{2+}]_i$ increase amounted to 491 nM. Bottom of columns, number of experiments. *N-Ac*, *N*-acetyl; *DH*, dihydro, *CP*, ceramide-1-phosphate; *C2-Cer*, C2-ceramide or *N*-acetyl-sphingosine. B, Concentration dependence of the inhibitory effect of SPPC (□) and GPS (○) on the KCl-induced $[Ca^{2+}]_i$ increase.

not activate $I_{K.DR}$ but rather decreased outward current (data not shown).

Inhibition of Ba^{2+} current in RINm5F cells by lysosphingolipids. To test the hypothesis that sphingolipids inhibit Ca^{2+} influx in RINm5F cells by blocking L-type Ca^{2+} channels, the effects of GPS, SPPC, and SPP on membrane Ba^{2+} currents were studied. Bath application of GPS (10 μM) reduced the amplitude of Ba^{2+} currents within seconds (Fig. 4A). Although the reversibility of this effect was generally poor, subsequent current block by Cd^{2+} was fully reversible. The current tracings displayed in Fig. 4, B and C, further illustrate the effect of GPS. Note that GPS did not accelerate or otherwise affect the inactivation time course of Ba^{2+} current during voltage-clamp steps. In nine cells, GPS reduced current amplitude at 0 mV from -13.8 ± 2.1 to -9.3 ± 1.6 pA/pF (Fig. 5A). This current decrease was significant within the voltage range from -30 to $+30$ mV. The extent of current inhibition by GPS was independent of the holding potential (fraction of control current at 0 mV: $71 \pm 5\%$ at V_H -80 mV versus $68 \pm 8\%$ at V_H -50 mV; four experiments; data not shown). The reversal potential was slightly shifted from $+42.6 \pm 2.5$ mV (control) to $+39.7 \pm 2.2$ mV (GPS, $p < 0.01$). Ba^{2+} current was half-activated at -13.7 ± 1.8 mV before and at -10.0 ± 1.7 mV ($p < 0.05$) after exposure to GPS; the slope of the conductance curves was not changed (6.6 ± 0.3 mV versus 6.9 ± 0.4 mV). Consistent with this shift, we found that the inhibitory action of GPS on Ba^{2+} current was potential dependent (Fig. 5B), being significantly more pronounced at -25 mV than at $+10$ mV (fraction of block: $51.4 \pm 6.6\%$ versus $29.3 \pm 3.8\%$, respectively; $p < 0.05$). The GPS-induced inhibition of Ba^{2+} current was concentration dependent (Fig. 5C). However, even at the highest concentration tested (20 μM), GPS did not abolish Ba^{2+} current.

Mechanism of Ba^{2+} current inhibition by lysosphingolipids in RINm5F cells. Sphingolipids apparently play a dual role in cellular regulation, acting as intracellular messengers and as ligands for plasma membrane receptors (Spiegel *et al.*, 1996; Meyer zu Heringdorf *et al.*, 1997). To distinguish between an intracellular and extracellular site of action, GPS (10 μM) was included in the pipette solution when measuring Ba^{2+} currents (Fig. 6A). As in time-matched controls, current amplitude measured at 0 mV increased rapidly to reach a stable level ~3 min after establishing the whole-cell mode. Thereafter, current remained unchanged for several minutes, regardless of the intracellular presence of GPS. On average, the voltage ramp-derived current-voltage relation obtained after 7.2 ± 1.2 min (nine experiments) of cell dialysis with GPS-containing pipette solution did not differ from that measured under control conditions (no GPS exposure) in a comparable group of cells (Fig. 6B). However, additional exposure of the cell to extracellular GPS led to a rapid current reduction. In all three cells exposed to extracellular GPS in addition to GPS in the pipette solution, current amplitude was reduced to an extent similar to bath-applied GPS only. These results indicate that the target for GPS and possibly other sphingolipids is at the outer face of the plasma membrane in RINm5F cells.

Sphingolipid-induced cellular responses in atrial myocytes, HEK 293 cells, HL-60 cells, and endothelial cells, for instance, are PTX sensitive (Okajima and Kondo, 1995; Bünemann *et al.*, 1996; Meyer zu Heringdorf *et al.*, 1996; van Koppen *et al.*, 1996a; 1996b), suggesting the involvement of G_i proteins in signal transduction. However, the sphingolipid-induced inhibition of the KCl-induced $[Ca^{2+}]_i$ increase was PTX-insensitive (Fig. 1), suggesting that G_i type G proteins do not participate. To study whether G proteins are involved at all in the sphingolipid actions in RINm5F cells, the cells were first dialyzed with guanine nucleotides included in the pipette solution before exposing the cells to GPS. With the stable GTP analog, GTPγS (100 μM), in the electrode solution, GPS caused a somewhat greater reduction of Ba^{2+} current than with control solution (Figs. 7A and 8). Similar results were obtained when the cells were dialyzed with GTP (100 μM) (Fig. 8). In contrast, the presence of the stable GDP analog, GDPβS (10 mM), in the pipette solution abolished the current reduction due to GPS (Figs. 7B and 8). A similar inhibitory effect was obtained with 1 mM GDPβS in the pipette solution. In the presence of 10 μM GPS, the

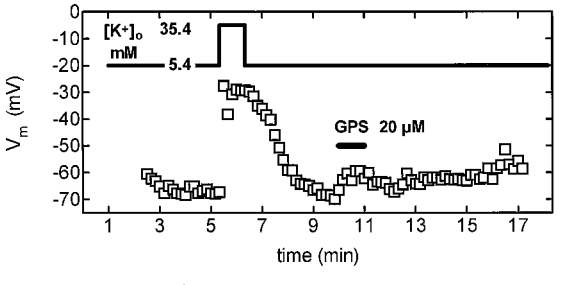

Fig. 3. Effects of high K^+ and GPS on membrane potential in RINm5F cells. Time course of membrane potential V_M in a representative RINm5F cell. With $[K^+]_o$ = 5.4 mM, V_M stabilized around -67 mV 3 min after patch disruption. Elevation of $[K^+]_o$ to 35.4 mM reversibly depolarized the cell to -30 mV, whereas GPS (20 μM) depolarized by <10 mV.

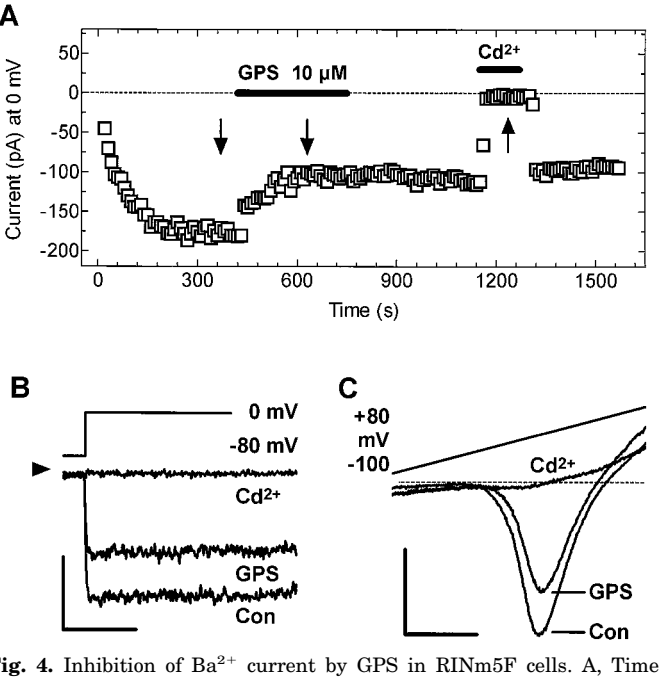

Fig. 4. Inhibition of Ba^{2+} current by GPS in RINm5F cells. A, Time course of voltage ramp-derived current measured at 0 mV in a typical cell. *Bars*, exposure to extracellular GPS (10 μM) and Cd^{2+} (200 μM). *Arrows*, times at which the current tracings displayed in B and C were recorded. B, Superimposed current tracings elicited by voltage steps to 0 mV before (*Con*) and after exposure to GPS and Cd^{2+}. *Arrowhead*, zero current level. *Calibration bars*, 100 pA, 100 msec. C, Superimposed current tracings in response to voltage ramps from -100 to $+80$ mV (duration, 400 msec) before (*Con*) and after exposure to GPS and Cd^{2+}. *Dashed line*, zero current level. *Calibration bars*, 100 pA, 50 mV.

fraction of control current measured at 0 mV with 10 and 1 mM GDPβS amounted to 97.3 ± 4.9% (nine experiments) and 90.2 ± 4.8% (eight experiments), respectively (data not shown). Control experiments with a Li_3PO_4 (10 mM)-containing electrode solution demonstrated that the block of the action of GPS is not due to Li^+, provided with GDPβS as trilithium salt (Fig. 8).

The effects of different compounds measured with different modes of application on Ba^{2+} currents in RINm5F cells are summarized in Fig. 8. Similar to GPS, bath application of SPPC (10 μM) reduced the current by ~35%, whereas SPP (10 μM) had no effect. The extent of current reduction caused by GPS and SPPC was similar to that induced by the α_2-adrenoceptor agonist clonidine (30 μM) (Schmidt *et al.*, 1991). The inhibitory effect of extracellular GPS was not mimicked by intracellular GPS and was fully prevented by intracellular application of GDPβS, whereas similar application of GTP and GTPγS slightly but not significantly increased the GPS-induced inhibition.

Inhibition of Ba^{2+} current in α_{1C}/β_3-expressing HEK 293 cells by GPS. The data presented so far suggest an extracellular target and participation of a G protein in the inhibitory effect of GPS in RINm5F cells. For comparison, we investigated the effects of GPS in HEK 293 cells stably expressing the human cardiac L-type Ca^{2+} channel α_{1C} subunit together with a β_3 subunit (Klöckner *et al.*, 1997). Ba^{2+} currents in these HEK 293 cells exhibited a bell-shaped current-voltage relation, with an activation threshold at −30 mV, a maximum between +10 and +20 mV, and current reversal between +50 and +60 mV (Fig. 9), which are properties typical for $I_{Ca,L}$. Similar to RINm5F cells, extracellular application of GPS (10 μM) significantly reduced the Ba^{2+} current in HEK 293 cells, by 53 ± 6% at maximum current (Fig. 9A). However, quite distinct from RINm5F cells, α_{1C}/β_3 subunit-expressing HEK 293 cells dialyzed with GPS (10 μM for 6 ± 1 min) in the electrode solution also exhibited a significant reduction in maximal current density compared with a control group, from −6.4 ± 1.0 to −3.6 ± 0.8 pA/pF (Fig. 9A). Furthermore, current amplitudes decreased continuously after entering the whole-cell configuration with intracellular GPS, whereas they increased and stabilized on a high level in time-matched controls (data not shown). The difference between RINm5F and HEK 293 cells was even more striking when the effect of the stable GDP analog GDPβS was analyzed. Although in RINm5F cells intracellular application of GDPβS abolished the inhibitory effect of

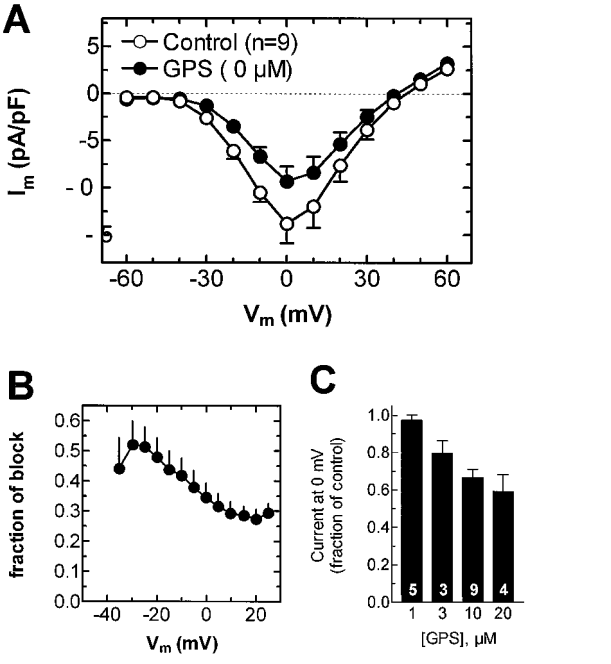

Fig. 5. GPS reduces Ba^{2+} current in RINm5F cells in a voltage- and concentration-dependent manner. A, Ramp-derived current-voltage relations in the absence (○) and presence (●) of 10 μM GPS. B, Fraction of blocked current as a function of clamp potential (data from A). Block became evident positive to −45 mV, reached a maximum around −25 mV, and declined toward more positive potentials. C, Average current at 0 mV in the presence of the indicated concentrations of GPS. Values are mean ± standard error; number of experiments is indicated.

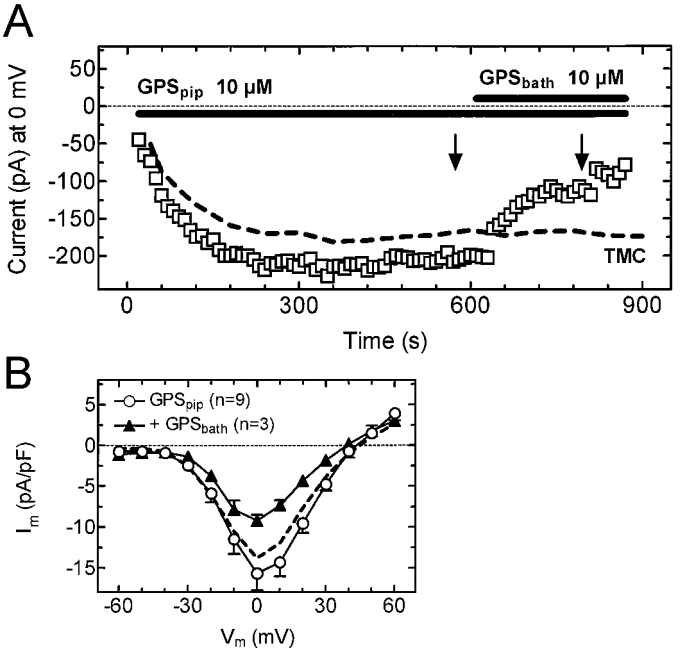

Fig. 6. Intracellularly applied GPS does not reduce Ba^{2+} current in RINm5F cells. A, Time course of current measured at 0 mV in a typical cell with 10 μM GPS in pipette solution (GPS_{pip}) and after additional bath application of GPS (GPS_{bath}). *Arrows*, times at which the curves displayed in B were recorded; *dashed line*, average current of time-matched controls (*TMC*). B, Average ramp-derived current-voltage relations measured after 7.2 ± 1.2 min of cell dialysis with 10 μM GPS in pipette solution (GPS_{pip}, ○, nine experiments) and after additional bath application of GPS (+GPS_{bath}, ▲, three experiments). *Dotted line*, control curve taken from Fig. 5A.

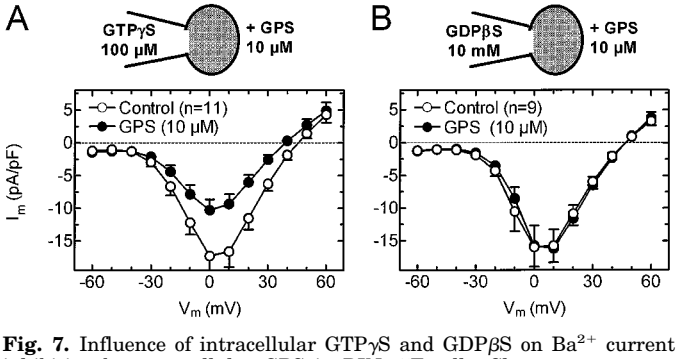

Fig. 7. Influence of intracellular GTPγS and GDPβS on Ba^{2+} current inhibition by extracellular GPS in RINm5F cells. Shown are average ramp-derived current-voltage relations in the absence (○) and presence (●) of 10 μM extracellular GPS with either GTPγS (100 μM, A) or GDPβS (10 mM, B) added to the electrode solution.

GPS, it had no effect on GPS-induced inhibition of Ba^{2+} currents in HEK 293 cells. As illustrated in Fig. 9B, when HEK 293 cells were first dialyzed with GDPβS (10 mM for 8 ± 1 min), Ba^{2+} current inhibition by extracellular GPS (10 μM) was similar to that in control cells. These results indicate that in HEK 293 cells stably expressing the pore-forming L-type Ca^{2+} channel α_{1C} subunit together with a β_3 subunit, both extracellular and intracellular GPS reduce Ba^{2+} currents and apparently without involvement of a G protein.

Discussion

The lysosphingolipids SPP and SPPC have been reported to cause a rapid increase in $[Ca^{2+}]_i$ in various cell types (Okajima and Kondo, 1995; Meyer zu Heringdorf *et al.*, 1996; 1997; Spiegel *et al.*, 1996; van Koppen *et al.*, 1996a, 1996b), apparently by activating G protein-coupled sphingolipid receptors. Therefore, we examined in the current study whether sphingolipids may regulate Ca^{2+} homeostasis in RINm5F insulinoma cells in a similar manner. The data presented herein demonstrate that sphingolipids elicit an opposite response in RINm5F cells (i.e., they inhibit Ca^{2+} transients, apparently by inhibiting Ca^{2+} entry through L-type Ca^{2+} channels). By testing a variety of different sphingolipids, we could demonstrate that the attenuation of depolarization-induced Ca^{2+} influx was restricted to certain compounds (i.e, GPS, PS, SPPC, and dihydro-SPPC), whereas various *N*-acylated sphingolipids and SPP had little or no effect. A similar pharmacological profile was obtained when measuring Ba^{2+} currents through L-type Ca^{2+} channels. GPS and SPPC inhibited the current, whereas SPP was without effect. The distinct effectiveness of some, but not all, sphingolipids studied, all of which consist of a long lipophilic hydrocarbon backbone and a hydrophilic head group, strongly argues against a nonspecific effect on the membrane lipid bilayer. Furthermore, preferential insertion of the amphiphilic lysosphingolipids into one leaflet of the lipid bilayer, thereby causing tension in the other leaflet and thus modulating channel activity (Martinac *et al.*, 1990), also is unlikely to be the mechanism by which these compounds inhibit Ca^{2+} currents. Such responses require tens of minutes to develop, whereas sphingolipid-induced inhibition of currents was observed within seconds. Finally, there is no evidence that Ca^{2+} current inhibition is due to a surface charge effect (Ji *et al.*, 1993) of the inhibitory sphingolipids because a small depolarization of membrane potential by GPS was measured (Fig. 3), which in fact may decrease channel availability rather than increasing it as theoretically expected for a positively charged compound.

Inhibition of KCl-induced $[Ca^{2+}]_i$ transients in intact RINm5F cells by the sphingolipids was more pronounced than the sphingolipid-induced inhibition of Ba^{2+} currents. For example, 10 μM GPS reduced the KCl-induced $[Ca^{2+}]_i$ increase by ~80%, whereas inhibition of maximal Ba^{2+} current was only 33%, suggesting that additional sites of action of GPS should be considered. However, first, GPS did not inhibit ryanodine receptor-mediated Ca^{2+} release, which may contribute to KCl-induced $[Ca^{2+}]_i$ increase in intact cells. Second, GPS did not lead to a hyperpolarization (Fig. 3), which could potentially counteract the KCl-induced depolarization and the consequent Ca^{2+} influx. The depolarization from −59 to −54 mV caused by GPS should result in a negligible reduction of Ca^{2+} channel availability (97.8% versus 96.6%; see Experimental Procedures), making a GPS-mediated inactivated state block highly unlikely. Third, a participation of low voltage-activated T-type Ca^{2+} channels in the KCl-induced Ca^{2+} influx and its inhibition by sphingolipids also is unlikely because (1) the L-type Ca^{2+} channel blocker verapamil completely prevented the KCl-induced Ca^{2+} influx and (2) only in a minor fraction of cells (17%) was some evidence obtained for the presence of T-type Ca^{2+} channels. Finally, it has to be considered that at the high extracellular K^+ concentration (35 mM) used for measurement of $[Ca^{2+}]_i$ transients in intact cells, the cells depolarized to only −30 mV (Fig. 3) and not to 0 mV, where the maximal Ba^{2+} current was observed. On the other hand, inhibition of Ba^{2+} current by GPS was shown to be potential dependent (i.e., maximal at ~−30 mV) (Fig. 5B). Thus, taking into account the different conditions to measure $[Ca^{2+}]_i$ transients and Ba^{2+} currents, the extent of inhibition by GPS (10 μM), ~80%

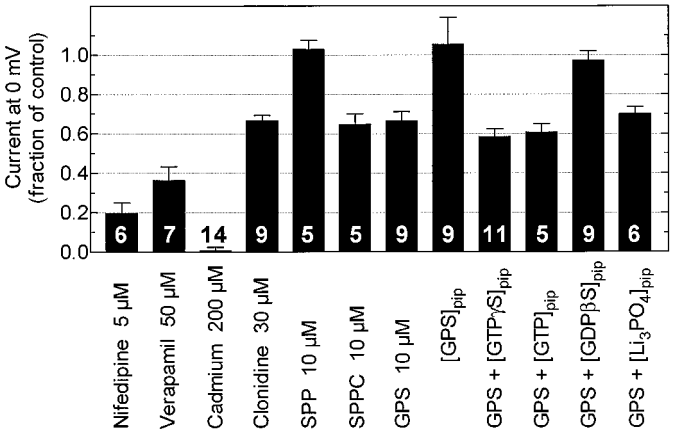

Fig. 8. Summary of effects of various agents on Ba^{2+} current in RINm5F cells. Current amplitude is expressed as fraction of control current at 0 mV. Values are mean ± standard error. *Bottom of columns*, number of experiments. Because control current amplitudes did not vary significantly between different experimental groups (Kruskal-Wallis test), pooled control currents (14.9 ± 1.0 pA/pF, 44 experiments) were taken to calculate the effect of GPS in the electrode solution ($[GPS]_{pip}$). All groups, except SPP, $[GPS]_{pip}$, and GPS + $[GDP\beta S]_{pip}$, were significantly different ($p < 0.05$) from their respective controls.

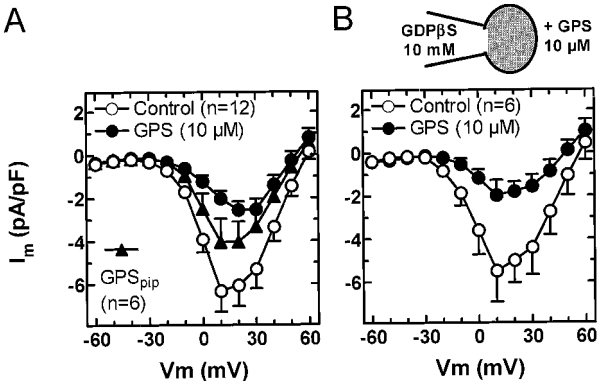

Fig. 9. Effects of GPS on Ba^{2+} current in HEK 293 cells expressing α_{1C} and β_3 Ca^{2+} channel subunits. A, Average step-derived current-voltage relations in the absence (○) and presence (●) of 10 μM extracellular GPS (12 experiments) and in cells dialyzed for 6 ± 1 min with 10 μM GPS (GPS_{pip}, ▲, six experiments). B, Average step-derived current-voltage relations in cells (six experiments) dialyzed for 8 ± 1 min with 10 mM GDPβS in the electrode solution before (○) and after (●) bath application of 10 μM GPS.

and ≥50%, respectively, is remarkably similar. Thus, we hypothesize that the sphingolipid-induced inhibition of depolarization-dependent $[Ca^{2+}]_i$ transients in RINm5F cells is, at least to a major extent, due to inhibition of L-type Ca^{2+} channels. Sphingolipids also have been shown to inhibit Ca^{2+} currents in two other cell types. In GH_4C_1 rat pituitary cells, SPPC (10 μM) was found to inhibit both Ca^{2+} currents and depolarization-induced Ca^{2+} influx, whereas SPP had no effect (Törnquist *et al.*, 1995). In rat ventricular myocytes, sphingosine (25 μM) greatly reduced Ca^{2+} current amplitude, whereas SPPC (25 μM) had no (McDonough *et al.*, 1994) or only a small inhibitory effect (Yasui and Palade, 1996).

Activation of muscarinic K^+ currents in atrial myocytes by SPP and SPPC apparently is mediated by a specific sphingolipid receptor coupled to G_i-type G proteins. The sphingolipid activation occurred at low nanomolar concentrations (EC_{50} = 1–2 nM), was completely blocked by PTX, was strictly GTP dependent, and was observed only when the sphingolipids were applied to the outer face of the membrane (Bünemann *et al.*, 1996; van Koppen *et al.*, 1996a). In comparison, the inhibitory sphingolipid action on Ca^{2+} entry in RINm5F cells was observed at micromolar concentrations and was PTX insensitive. Furthermore, inhibition of Ca^{2+} current by GPS did not require the addition of GTP. However, application of the stable GDP analog GDPβS into the cell interior completely abolished the GPS-induced inhibition, suggesting that a guanine nucleotide-sensitive target, most likely a G protein, is involved in the inhibitory sphingolipid action. The data, furthermore, suggest that endogenous GTP required for activation of the responsible G protein or proteins is present in sufficient amounts under the whole-cell condition used to measure Ca^{2+} currents. To study a possible involvement of a membrane receptor, GPS was applied either extracellularly or intracellularly. We demonstrate that only extracellular application of GPS induced inhibition of Ca^{2+} currents in RINm5F cells, whereas intracellularly applied GPS had no effect and also did not alter Ca^{2+} current inhibition induced by extracellular GPS. These data suggest that Ca^{2+} current inhibition caused by GPS in RINm5F cells is not due to direct activation of the responsible G proteins, which should be located on the inner surface of the membrane, but is mediated by a target facing the extracellular space, such as a membrane receptor.

To corroborate the hypothesis that RINm5F cells express a sphingolipid receptor mediating a G protein-dependent inhibition of Ca^{2+} current, we studied the effect of GPS on Ca^{2+} currents in HEK 293 cells stably expressing the human cardiac L-type Ca^{2+} channel α_{1C} subunit together with a β_3 subunit (Klöckner *et al.*, 1997). GPS inhibited Ca^{2+} currents in these cells at least as well as in RINm5F cells. In contrast, however, to the data obtained in RINm5F cells, the inhibitory effect of GPS in HEK 293 cells was observed regardless of which side of the membrane was exposed to GPS. Moreover, the GPS-induced inhibition of Ca^{2+} currents in HEK 293 cells was not affected by GDPβS. It must be noted here that the HEK 293 cells express a different pore-forming L-type Ca^{2+} channel subunit (α_{1C}) than the neuroendocrine RINm5F cells (α_{1D}), which in addition are equipped with the complete set of subunits forming the native L-type Ca^{2+} channel (Birnbaumer *et al.*, 1994). Thus, the minimal conclusion derived from these data is that HEK 293 cells do not express a receptor for GPS mediating via a G protein inhibition of the L-type Ca^{2+} channel composed of α_{1C} and β_3 subunits. The Ca^{2+} current inhibition caused by GPS in HEK 293 cells may be due to a direct effect of the sphingolipid on the α_{1C} or β_3 subunits (or both). Thus, to prove this hypothesis, it may be necessary to express the complete neuroendocrine type of L-type Ca^{2+} channel with all of its subunits in a suitable host cell and then study its regulation by sphingolipids.

We can only speculate about the G protein type apparently involved in the inhibitory sphingolipid signaling in RINm5F cells. These cells possess G_i and G_o proteins, which are both activated by α_2-adrenoceptors and couple to L-type Ca^{2+} channels in an inhibitory manner (Schmidt *et al.*, 1991). However, these G proteins are PTX sensitive and therefore not suited to serve as transducers for putative lysosphingolipid receptors in RINm5F cells. Most, if not all, voltage-dependent Ca^{2+} channels underlie G protein regulation via membrane-delimited or second messenger-dependent mechanisms (Wickman and Clapham, 1995). Thus, for example, one might speculate that $\beta\gamma$ subunits released from a PTX-insensitive G protein could carry the signal for inhibition of Ca^{2+} current as suggested for various channels (Wickman and Clapham, 1995; Qin *et al.*, 1997).

In conclusion, we demonstrate in the current study that certain lysosphingolipids markedly inhibit influx of Ca^{2+} through L-type Ca^{2+} channels into RINm5F insulinoma cells and provide circumstantial evidence that this inhibitory sphingolipid action involves a PTX-insensitive G protein and an extracellular target structure, probably a membrane receptor.

Acknowledgments

We thank Doris Petermeyer for expert technical assistance, Dr. G. Schultz for providing the RINm5F-cells, and Drs. J. Eisfeld, U. Klöckner, A. Schwartz, and G. Varadi for the HEK 293 cells expressing the α_{1C} and β_3 Ca^{2+} channel subunits.

References

Ashcroft FM and Rorsman P (1989) Electrophysiology of the pancreatic β-cell. *Prog Biophys Mol Biol* **54:**87–143.

Bennett DL, Cheek TR, Berridge MJ, De Smedt H, Parys JB, Missiaen L, and Bootman MD (1996) Expression and function of ryanodine receptors in nonexcitable cells. *J Biol Chem* **271:**6356–6362.

Birnbaumer L, Campbell KP, Catterall WA, Harpold MM, Hofmann F, Horne WA, Mori Y, Schwartz A, Snutch TP, Tanabe T, and Tsien RW (1994) The naming of voltage-gated calcium channels. *Neuron* **13:**505–506.

Bünemann M, Liliom K, Brandts B, Pott L, Tseng JL, Desiderio DM, Sun G, Miller D, and Tigyi G (1996) A novel membrane receptor with high affinity for lysosphingomyelin and sphingosine-1-phosphate in atrial myocytes. *EMBO J* **15:**5527–5534.

Choi OH, Kim J, and Kinet J (1996) Calcium mobilization via sphingosine kinase in signalling by the FcεRI antigen receptor. *Nature (Lond)* **380:**634–636.

de Waard M, Gurnett CA, and Campbell KP (1996) Structural and functional diversity of voltage-activated calcium channels. *Ion Channels* **4:**41–87.

Findlay I and Dunne MJ (1985) Voltage-activated Ca^{2+} currents in insulin-secreting cells. *FEBS Lett* **189:**281–285.

Ghosh TK, Bian J, and Gill DL (1994) Sphingosine-1-phosphate generated in the endoplasmic reticulum membrane activates release of stored calcium. *J Biol Chem* **269:**22628–22635.

Hannun YA and Bell RM (1987) Lysosphingolipids inhibit protein kinase C: Implications for the sphingolipidoses. *Science (Washington DC)* **235**:670–674.

Ji S, Weiss JA and Langer GA (1993) Modulation of voltage-dependent sodium and potassium currents by charged amphiphiles in cardiac ventricular myocytes: effects via modification of surface potential. *J Gen Physiol* **101:**355–375.

Klöckner U, Mikala G, Eisfeld J, Iles DE, Strobeck M, Mershon JL, Schwartz A, and Varadi G (1997) Properties of three COOH-terminal splice variants of a human cardiac L-type Ca^{2+}-channel α_1-subunit. *Am J Physiol* **272:**H1372–H1381.

Martinac B, Adler J, and Kung C (1990) Mechanosensitive ion channels of *E. coli* activated by amphipaths. *Nature (Lond)* **348:**261–263.

Mattie ME, Brooker G, and Spiegel S (1996) Sphingosine-1-phosphate, a putative second messenger, mobilizes calcium from internal stores via an inositol trisphosphate-independent pathway. *J Biol Chem* **269:**3181–3188.

McDonough PM, Yasui K, Betto R, Salviati G, Glembotski CC, Palade PT, and Sabbadini RA (1994) Control of cardiac Ca^{2+} levels: inhibitory actions of sphin-

gosine on Ca^{2+} transients and L-type Ca^{2+} channel conductance. *Circ Res* **75:**981–989.
Meyer zu Heringdorf D, van Koppen CJ, and Jakobs KH (1997) Molecular diversity of sphingolipid signalling. *FEBS Lett* **410:**34–38.
Meyer zu Heringdorf D, van Koppen CJ, Windorfer B, Himmel HM, and Jakobs KH (1996) Calcium signalling by G-protein-coupled sphingolipid receptors in bovine aortic endothelial cells. *Naunyn-Schmiedebergs Arch Pharmacol* **354:**1–7.
Okajima F and Kondo Y (1995) Pertussis toxin inhibits phospholipase C activation and Ca^{2+} mobilization by sphingosylphosphorylcholine and galactosylsphingosine in HL60 leukemia cells: implications of GTP-binding protein-coupled receptors for lysosphingolipids. *J Biol Chem* **270:**26332–26340.
Olivera A and Spiegel S (1993) Sphingosine-1-phosphate as second messenger in cell proliferation induced by PDGF and FCS mitogens. *Nature (Lond)* **365:**557–560.
Qin N, Platano D, Olcese R, Stefani E, and Birnbaumer L (1997) Direct interaction of $G\beta\gamma$ with a C-terminal $G\beta\gamma$-binding domain of the Ca^{2+} channel α_1 subunit is responsible for channel inhibition by G protein-coupled receptors. *Proc Natl Acad Sci USA* **94:**8866–8871.
Schmidt A, Hescheler J, Offermanns S, Spicher K, Hinsch KD, Klinz FJ, Codina J, Birnbaumer L, Gausepohl H, Frank R, Schultz G, and Rosenthal W (1991) Involvement of pertussis toxin-sensitive G-proteins in the hormonal inhibition of dihydropyridine-sensitive Ca^{2+}-currents in an insulin-secreting cell line (RINm5F). *J Biol Chem* **266:**18025–18033.
Sharp GWG (1997) Mechanisms of inhibition of insulin release. *Am J Physiol* **271:**C1781–C1799.
Spiegel S, Foster D, and Kolesnick R (1996) Signal transduction through lipid second messengers. *Curr Opin Cell Biol* **8:**159–167.
Törnquist K, Pasternack M, and Kaila K (1995) Sphingosine derivatives inhibit depolarization-evoked calcium entry in rat GH_4C_1 cells. *Endocrinology* **136:**4894–4902.
van Koppen CJ, Meyer zu Heringdorf D, Laser KT, Zhang C, Jakobs KH, Bünemann M, and Pott L (1996a) Activation of a high affinity G_i protein-coupled plasma membrane receptor by sphingosine-1-phosphate. *J Biol Chem* **271:**2082–2087.
van Koppen CJ, Meyer zu Heringdorf D, Zhang C, Laser KT, and Jakobs KH (1996b) A distinct G_i protein-coupled receptor for sphingosylphosphorylcholine in human leukemia HL-60 cells and human neutrophils. *Mol Pharmacol* **49:**956–961.
Wickman KD and Clapham DE (1995) G-protein regulation of ion channels. *Curr Opin Neurobiol* **5:**278–285.
Yasui K and Palade P (1996) Sphingolipid actions on sodium and calcium currents of rat ventricular myocytes. *Am J Physiol* **270:**C645–C649.

Send reprint requests to: Dr. Karl H. Jakobs, Institut für Pharmakologie, Universitätsklinikum Essen, Hufelandstrasse 55, D-45122 Essen, Germany.